

“Flight Template”

A tool for the optimization of sailplane aerodynamics for cross country flight at the preliminary design stage

Matthieu Scherrer
Toulouse – France
matthieu.scherrer@free.fr

Abstract

A new tool for the aerodynamic optimization of a sailplane wing is proposed in order to take the specificity of a typical cross country flight into account during the preliminary design stage. It is called “Flight Template”, because it embodies the statistical aspect of real flight. The statistical “Flight Spectrum” acts as a filter of aerodynamic wing characteristics and helps define a realistic cost function reflecting global performance for multiple-point optimization. The concept of Flight Template is presented, and a methodology is proposed to determine it experimentally. Some documented examples are given. In addition, applications of the Flight Template tools in preliminary design process are presented. Illustrations of the use of Flight Template are given for airfoil selection, planform optimization, and airfoil numerical optimization.

Nomenclature

C_L	=	lift coefficient
C_D	=	drag coefficient
AR	=	Aspect ratio
ϕ	=	bank angle
$\dot{\Psi}$	=	heading scrolling in turn

Introduction

The numerical optimization of a sailplane wing is a real challenge to put in equations and figures. Contrary to airliners that are designed for a single cruise condition, sailplanes are flown over a large range of speed and lift coefficients. Thus, a relevant performance figure is more difficult to define for sailplanes.

When applying a single point classical process for one lift coefficient, optimization leads to a radical design that is not adapted to a wide speed range. The goal of the “Flight Template” defined here is to define an aerodynamic optimization process representative of the conditions actually encountered by sailplanes during cross country flights. It will provide a weighting of performance as function of C_L that can be used simply.

Part 1: Flight Template Concept

Theoretical background

For gliding, a sailplane extracts power from gravity. It is brought back to the ground due to the work of drag. Considering this, we shall search for the design that minimizes the power absorbed by drag over the whole flight duration. This will be the starting point for defining a cost function.

Elementary work dE absorbed by drag D during a short period dt can be written as:

$$dE = D \times V dt = 1/2 \rho S V^3 C_D dt$$

The normalized mean power \bar{P} absorbed by drag force during a flight period T is proportional to the sum of the elementary work over the flight, as follows:

$$\bar{P} = \frac{\int dE}{T} = \frac{\rho S}{2T} \int_{\text{Flight}} C_D(t) V^3(t) dt \quad (1)$$

By mathematical operation (see Appendix), the integral over the flight duration can be transformed into one over the C_L range:

$$\bar{P} = \frac{\rho S}{2} \int_{C_L \text{ range}} C_D(C_L) V^3(C_L) f_t(C_L) dC_L$$

$$\text{with } \boxed{f_t(C_L) = \frac{1}{T} \frac{d\tilde{t}}{dC_L}(C_L)} \quad (2)$$

A function $f_t(C_L)$ is defined (Eq 2), and is called the “Flight Template”. It corresponds to the C_L spectrum over the flight for one given C_L , the value of $f_t(C_L)$ represents the density of time spent at this C_L condition.

What is needed for building this function is a discrete recording of C_L history over the flight. Note that Flight Template must be “normalized”. At the end of the process, we should have:

$$\int_{C_L \text{ range}} f_t(C_L) dC_L = 1 \quad (3)$$

Definition of an aerodynamic cost function

If the flight is quasi steady, that is “little maneuvering is performed”, C_L and speed V are correlated through the following relation:

$$V = \sqrt{Nz} \frac{V_1}{\sqrt{C_L}} \quad (4)$$

where V_1 and Nz are computed from:

$$V_1\left(\frac{m}{S}, h\right) = \sqrt{\frac{2g}{\rho(h)} \frac{m}{S}} \quad (5)$$

$$Nz = \frac{1}{\cos\phi} = \sqrt{1 - \left(\frac{V\dot{\Psi}}{g}\right)^2} \quad (6)$$

V_1 is a function of wing loading and pressure altitude, and Nz is computed from the path. Here ϕ is bank angle, and $\dot{\Psi}$ is heading scrolling in turn. This case corresponds to the classical steady level flight of a sailplane, as well as to thermalling.

The mean power \bar{P} absorbed by drag force during the flight period then is expressed by:

$$\bar{P} = \frac{\rho S V_1^3}{2} \times \left(\overline{\frac{C_D}{C_L^{3/2}}} \right)$$

This indicates that a driving parameter from an aerodynamic point of view, weighted by the C_L history, is the following product:

$$\left(\overline{\frac{C_D}{C_L^{3/2}}} \right) = \int_{C_L \text{ range}} \frac{C_D(C_L)}{C_L^{3/2}} f_t(C_L) dC_L \quad (7)$$

Here the Flight Template implicitly translates drag time history during a flight in terms of a weighted aerodynamic coefficient. This quantity must be minimized, and is a simple and interesting cost function within a numerical optimization loop.

Determination of Flight Templates from GPS recording

For defining a relevant cost function, the Flight Template must be representative of real flights. A strategy of determination, from GPS flight logger, was developed and applied.

GPS devices are widely used for navigation and flight recording in the gliding community. A large flight recording database is easily available on the Internet (see www2.onlinecontest.org, for instance). Knowing the weight of the glider, V_1 can be computed (see Eq. (5)), and the path can be post-processed to obtain the C_L history of the flight (from Eq (4)). From this C_L history, the C_L spectrum of the recording can be determined.

IGC files provide raw information from the flight logger, post-processing must be performed to get C_L history from the flight path. The following operation must be implemented:

- Filter position signal and ground velocity vector \mathbf{V}
- Evaluate mean wind vector \mathbf{W}
- Evaluate load factor Nz using Eq. (6)
- Then compute C_L using Eq. (4)

Such a program has been written, and many flight paths processed to create a Flight Template data bank.

Selected examples of Flight Templates

From each flight recording, a specific Flight Template can be produced. The detail of one Flight Template is dependent on the specific pilot, meteorological condition etc.; therefore, some specific examples that have been studied are presented.

The three flights displayed here were all performed from French gliding center, CNVV, in St Auban. The pilot was Denis Guerin and the glider a Ventus 2a (contest number: EQ). All three flights were performed over the same mountainous region. On a typical day in this region, strong thermals and ridge lines require little circling time. Three successive days were recorded. The wing loadings for the three flights are, respectively, 34, 40 and 47 kg/m².

Airspeed spectrum analysis

The airspeed spectrum represents the time spent at each speed of the speed polar. On Fig. 1 it is shown that all three flights were performed over a rather large speed range:

- The first flight was the shortest test flight in term of covered distance. It was performed at the lightest wing loading on a poor day and is also the slowest (the airspeed range is to the left in the figure).
- The second flight was performed with heavier wing loading. Two speeds are notable, that corresponding to circling (105km/h) and that for straight flight (155km/h).
- The third flight corresponds to the maximum distance covered. It was performed at wing loading close to maximum, in good soaring weather. The mean speed is the fastest and the little circling time at the low speed peak is reduced.

Flight Template analysis

In term of the " C_L spectrum" the situation is quite different from the airspeed spectrum. Flight Templates resulting from those three flights are shown in Fig. 2.

It can be observed that for the three flights presented here, which were quite different flights, Flight Templates are quite close at the end. They all three present a peak around $C_L = 0.4-0.5$, meaning this lift coefficient is the most used during flight.

The transcription from speed to C_L takes into account the wing loading. Wing loadings were quite different for the three flights presented. This, rather than the C_L 's, is why the speed spectrums differ so much.

Comment

It seems that the pilot uses the sailplane, from an aerodynamic point of view (i.e. lift coefficient), always in a similar way.

From a handling point of view, this corresponds to using the same flap setting and pitch attitude, independent of the wing loading. This would mean an experienced pilot seems to drive the glider to reach a specific aerodynamic conditions on the wing.

This conclusion can be generalized to a wide number of cross country flights.

Envelope Flight Template strategy

It was shown that each flight produces a specific Flight Template. However, while studying a large set of GPS recordings, it was found that the different Flight Templates always have similar characteristics.

For preliminary design use, it is interesting to have one single reference Flight Template. Flight for various glider pilots, wing loadings and weather conditions were considered.

An “Envelope Flight Template” was derived from current experience dealing with flight post processing (See Fig. 3 and Table 1). The envelope obtained represents a statistically relevant aerodynamic history of cross-country flights for current sailplanes in Europe. This Envelope Flight Template is an interesting tool for sailplane preliminary design, and is easy to use.

Example of the use of the Envelope Flight Template is now detailed.

Part 2: Using Flight Templates

In parallel to this theory, simple but accurate computational tools were developed in order to evaluate the feasibility of an optimization scheme as proposed. Documented examples are now detailed.

Envelope Flight Template used as “Polar filter”

The drag polar is a key element for airfoil selection. Airfoils can be compared according to different criteria, as for instance their minimum drag C_{Dmin} or their maximum lift C_{Lmax} . For a sailplane, the whole evolution of C_D versus C_L is to be considered.¹

Some results of XFOIL calculations² for five existing sailplane airfoils with number of Reynolds varying along the polar ($Re * \sqrt{C_L} = 1.250 * 10^6$) are presented in Fig. 4. Airfoil coordinates used for this study were either public or evaluated from photos, with no guarantee of accuracy.

The Flight Template is used as a multiplying filter on $C_D/C_L^{3/2}$ as a function of C_L . This creates the function to be summed for computing $\left(\frac{C_D}{C_L^{3/2}}\right)$ (ref. to Eq. (7))

This manipulation highlights certain part of the polar. It helps find where the differences between the airfoils most affect the performance from an operational point of view.

From Fig. 5 we may observe that $C_D/C_L^{3/2}$ curves are different at high C_L values, and are difficult to compare at $C_L \sim 0.4$. When weighted using the envelope Flight Template (Fig. 6.), the high C_L region is somewhat flattened, whereas $C_L \sim 0.4$ region is magnified. This gives details on the differences that influence the most global airfoil performance.

Summing this weighted $C_D/C_L^{3/2}$ with respect to C_L gives $\left(\frac{C_D}{C_L^{3/2}}\right)$ (refer to Eq (7)). This figure is directly

proportional to the power absorbed by the airfoil drag during a typical cross country flight performed according to the Envelope Flight Template program.

Results for the tested airfoils are presented below:

Airfoil	$\left(\frac{C_D}{C_L^{3/2}}\right)$
HQ-300GD-mod2 (public coord.)	0.01640365
FX S 02-196 (public coord.)	0.01731888
OAP1 (coord. from photo)	0.01620513
Eppler E603 (public coord.)	0.01638561
Discus (coord. from photo)	0.01467457

According to the criterion developed in this paper, the Discus airfoil is the best suited for minimizing the power absorbed by airfoil drag during a typical cross country flight. The relatively low C_{Lmax} level, compared to the other airfoils, does not appear to affect the overall performance determined by the current weighting.

Note that the weighting defined here highlights the ability to minimize power absorbed by drag, and not ability to climb (Discus, which is used in developing this theory, is sometimes stated as not an easy climber, and needs some training to get the full benefit of its performance). That is probably why the weighting of high C_L region is so much less.

Envelope Flight Template for plan-form optimization

Aspect ratio selection is also a key factor in sailplane design. For Standard and 15m classes, the aspect ratio must be optimized with fixed span. This is a multidisciplinary topic (aerodynamics and structures), and the Flight Template gives relevant insights into the aerodynamics aspects.

Calculations were performed on different wings for a given airspeed ($V = 35\text{m/s}$). The baseline plan form is the Discus wing, and homothetic transformation was applied to vary the aspect ratio and surface for a given span (Fig. 7).

An extended lifting line³ was used to compute induced drag and derive local airfoil drag of those geometries (Fig. 8). This computation method is refined enough for capturing the effects of the Reynolds number variation along the span. It is also quick enough for computing many configurations within a short period.

The drag decomposition presented in Fig. 9 shows an expected result. It is known¹ that increasing aspect ratio results in a decrease in C_{Di} at given C_L , whereas it increases $C_{Dairfoil}$ (considering a fixed span $b = 15\text{m}$).

Using the Flight Template as a filter, a relevant cost function is easy to compute for general geometries. The trend seems to be that there is an aerodynamic optimum at around $AR = 30$ (also, the optimum is within 1% for $AR = 27.5$). This is an optimum in terms of minimum power absorbed by drag during a cross country flight.

$AR = 30$ is quite a high value for Standard class sailplanes, and therefore, there is the possibility for aerodynamic gains with greater aspect ratios. Nevertheless, consideration such as landing speed (which is directly related to wing area), may constrain this optimum for the Standard class.

On the other hand, $AR = 27$ corresponds to a common value in 15m class. In this case, flap help at reducing speed in landing configuration even with reduced wing area.

The Envelope Flight Template for the numerical optimization of airfoils

The Flight Template can also be used within automated conception loops. An optimization program has been written for optimizing three airfoils parameters at the same time. The objective of this program is to minimize the cost function defined using Flight Template (see Fig. 11). This was mainly an attempt to demonstrate the optimization process in order to evaluate its feasibility.

Once again the Discus airfoil was chosen as the reference. The degrees of freedom to be optimized were simple and physical. The airfoil was defined through the definition of maximum camber, position of maximum camber, and position of maximum thickness. The relative thickness of the airfoil was considered to be a constraint.

Other degrees of freedom defining the airfoil can be defined⁴ and would provide a more refined optimization process.

For creating a new geometry, the original airfoil was perturbed, and an unconstrained optimization process was performed.

The objective was to minimize $\left(\frac{C_{DAirfoil}}{C_{LSailplane}^{3/2}}\right)$. The

optimization algorithm has used both global and local optimization method for converging up to the minimum of the objective function. It was necessary to perform 40 iterations in order to satisfy the convergence criteria, accounting for 90 evaluations of the objective function.

As a result of the optimization, the cost function was reduced by 1%.

The geometry created by the optimizer is plotted on Fig. 12 and compared with the original. Main characteristics of the airfoils are given below:

	Original Airfoil	Modified Airfoil
Relative thickness	15.80%	15.80%
Position of maximum thickness	41.00%	33.60%
Relative camber	3.71%	3.29%
Position of maximum camber	45.30%	43.80%
$\left(\frac{C_D}{C_L^{3/2}}\right)$	0.01467457	0.01452589

The polar of the resulting airfoil is displayed in Fig. 13 along with the original. The modified airfoil has a less pronounced drag bucket. There is a loss at the lower and upper end of the drag bucket when compared to the polar of the original airfoil.

The drag rise for the new airfoil also occurs at a higher C_L than for the original. This gain for the high C_L values compensates the loss of laminarity for lower C_L when considering the cost function as a relevant measurement for performance.

When detailing the weighted $C_D/C_L^{3/2}$ curves (Fig. 14), we observe an exchange of performance between high C_L and low C_L region. This exchange seems beneficial for the cost function used here.

As a result from the optimization, there is a gain with respect to the Discus airfoil, which was considered the most suitable among the airfoils available. It is also noteworthy that the optimized airfoil has a geometry and a drag polar quite different from the original airfoil. This means that these two different airfoils concepts provide a competitive efficiency during a cross country flight.

Note that for a given $\left(\frac{C_D}{C_L^{3/2}}\right)$, airfoil selection can be

performed on other parameters. For instance, pitching moment for the modified airfoil is reduced by 12%, which is of interest for an optimization with a pitching moment constraint (trim drag modeling).

The C_{Lmax} can also be an important issue, since it is linked to the ability to climb.

Conclusions

The so called “Flight Template” concept, developed in this paper, is a promising tool for the preliminary design of sailplanes. It is a simple filter of aerodynamic characteristics. It helps sorting aerodynamics design, by taking into account the specifics of a cross-country flight by the definition of a global performance cost function.

Its use within numerical optimization schemes has been evaluated and is even more promising. The aerodynamic performance can be optimized in itself, as initiated in this paper, for an airfoil. An integration of the aerodynamic performance within a Multi-Disciplinary Optimization process is easy to imagine. The definition of the global cost function enables an easy integration of aerodynamic performance within a set of constraint from different disciplines.

Acknowledgments

I want to thank all the reviewers who took the time to consider my writings. They were involved from the earliest stages of developing this theory to the final stages of writing of this OSTIV paper. Special thanks go to Jean-Luc Delort, François Lorrain, Stephan Aubin and Jean-Paul Pinacho for their help and feedback.

References

- ¹Thomas F, “Fundamental of Sailplane Design”, College park press.
- ²Drela M, An Analysis and Design System for Low Reynolds Number Airfoils (Xfoil). *Lecture Notes in Engineering: Low Reynolds Number Aerodynamics*, T. J. Mueller (ed.), Vol. 54, Springer-Verlag, New York, June 1989, pp. 1-12
- ³James C. Sivells & Robert H. Neely, “Method for calculating wing characteristics by lifting-line theory using nonlinear section lift data”, NACA TN 1269 Apr 1947.
- ⁴Drela M, “Pro and cons of airfoil optimization”, in *Frontiers of Computational Fluid Dynamics* (1998)
- ⁵L.M.M. Boermans and G Waibel “Aerodynamic design of the standard class sailplane ASW-24”, *Technical Soaring*, Vol. 13, No. 3, 1989, page 72

⁶F.X. Wortmann, "A critical Review of the Physical Aspect of Airfoil Design at Low Reynolds Number", NASA. CR2315, Nov. 1973

⁷L.M.M. Boermans and H.J.W Selen "On the Design of Some Airfoils for Sailplane Application", TU-Delft report LR-326 (April 1981).

⁸L. M. M. Boermans and A van Garrel "Design and Windtunnel Test Results of a Flapped Laminar Flow Airfoil for High Performance Sailplane Application" ICAS-94-5.4.3, Anaheim, Sept. 1994.

⁹M. Drela, "Element of Airfoil Design Methodology", *Progress in Astronautics and Aeronautics: Applied Computational Aerodynamics*, Vol. 125, AIAA, pp. 167--189.

¹⁰M. A. Gomez-Tierno, J. J. Martinez Garcia & E Garcia-Julia, "A universal Dimensionless Model for the McCready Sailplane Theory", *Proc Instn Mech Engrs*, Vol. 213, Part G.

¹¹D E Metzger and J K Hedrick, "Optimal Flight Paths for Soaring Flight". *J. Aircrafts*, Vol. 12, No. 11, Nov 1975

Appendix :

Mathematical handling for getting Flight Template from discrete C_L history

In Eq. (1), mean power absorbed by drag is basically expressed as the integral over the duration of the flight:

$$\bar{P} = \frac{\int dE}{T} = \frac{\rho S}{2T} \int_{\text{Real flight}} C_D(t) V^3(t) dt$$

At first, it is necessary to re-order the flight samples: we shall sort them according to increasing C_L . This manipulation does not change the value of the mean power, which is still equal to:

$$\begin{aligned} \bar{P}_{\text{Real flight}} &= \bar{P}_{\text{Re-ordered flight}} \\ &= \frac{\rho S}{2T} \int_{\text{Re-ordered flight}} C_D(\tilde{t}) V^3(\tilde{t}) d\tilde{t} \end{aligned}$$

Then a single value of re-ordered time sample corresponds to a single value of C_L , and vice versa.

$$C_L = g(\tilde{t}) \Leftrightarrow \tilde{t} = g^{-1}(C_L)$$

This was not the case in the initial, unordered, real flight recording

Now we can perform the change in variable within the integral. That is, we consider C_D as a function of C_L history instead of time history. We have to do the following manipulation for evaluating the mean power \bar{P} :

$$\frac{1}{T} d\tilde{t} = \frac{1}{T} \frac{d\tilde{t}}{dC_L} (C_L) dC_L = f_i(C_L) dC_L$$

Then appears the "Fight Template" $f_i(C_L)$. This function accounts for the normalized time $\frac{d\tilde{t}}{T}$ spent by the sailplane during the flight at a C_L contained within C_L range $[C_L - dC_L/2, C_L + dC_L/2]$.

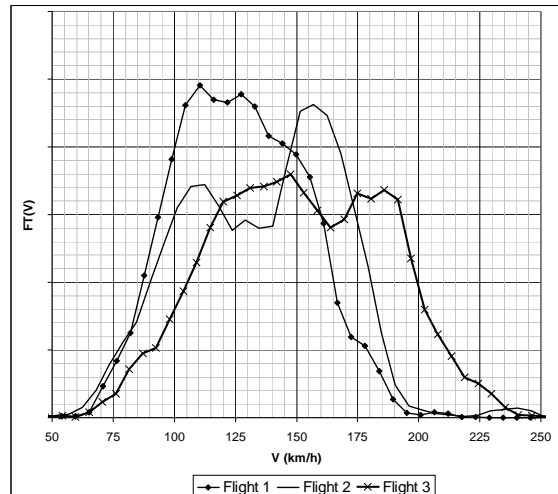


Figure 1 Speed spectrum for the three detailed flights.

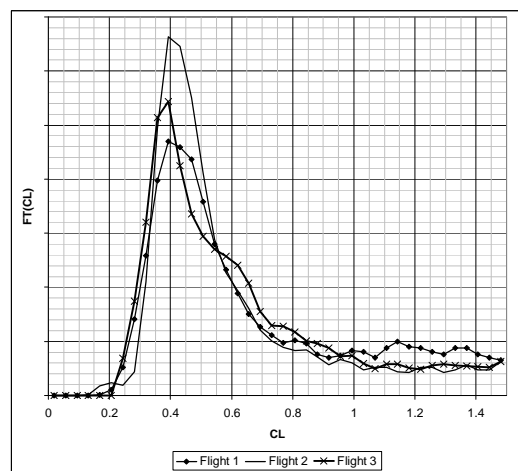


Figure 2 Flight templates for the three detailed flights.

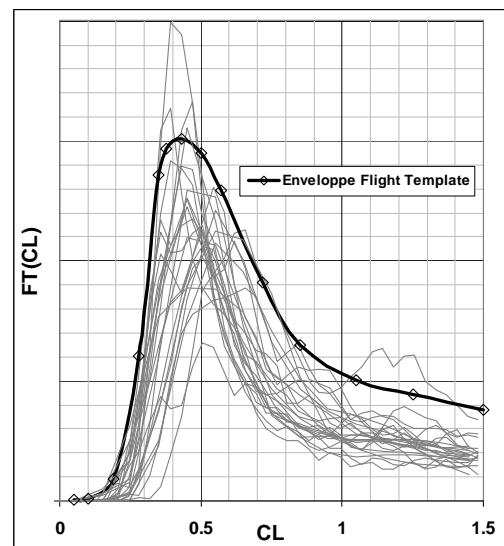


Figure 3 Envelope Flight Template.

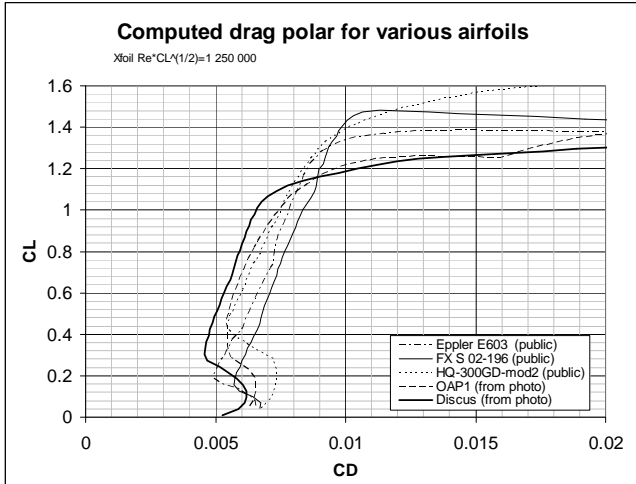


Figure 4 : Calculated drag polars for five samples airfoils.

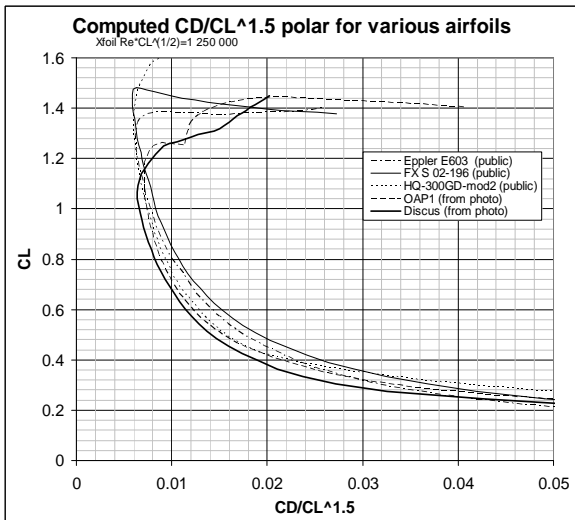


Figure 5 Calculated $C_D/C_L^{1.5}$ polars for the same five samples airfoils

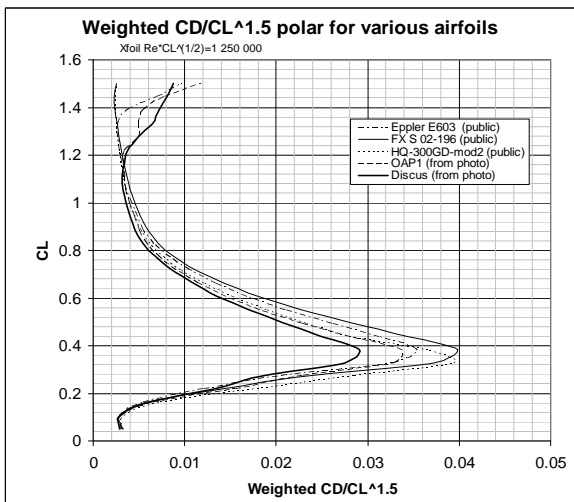


Figure 6 Weighted $C_D/C_L^{1.5}$ polars for the same five samples airfoils



Figure 7 Discus wing plan-form, and homothetic versions.

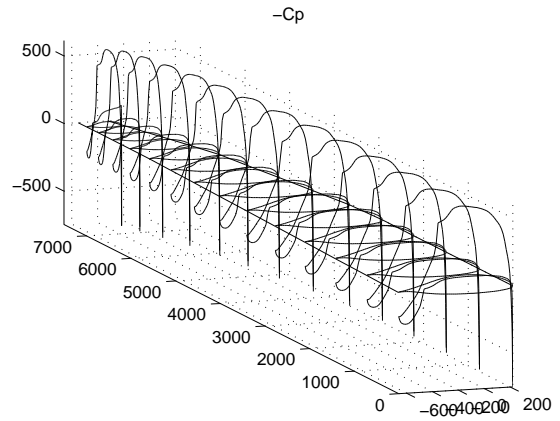


Figure 8 The extended lifting-line theory computes local behavior of each airfoil, and induced drag.

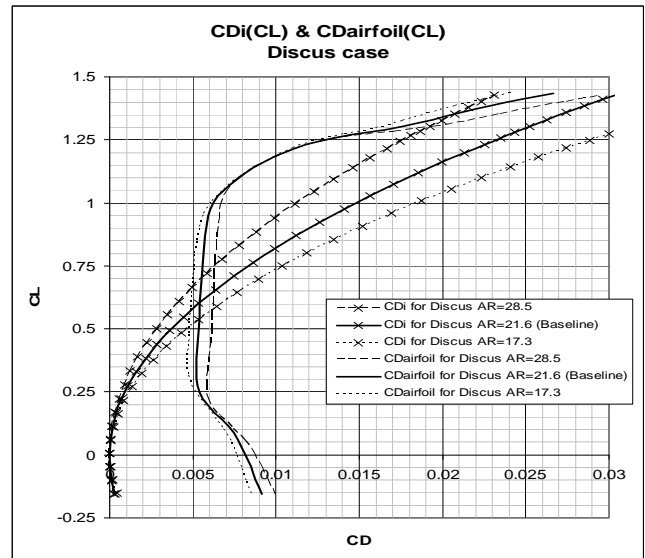


Figure 9 Wing drag decomposition, for various planforms.

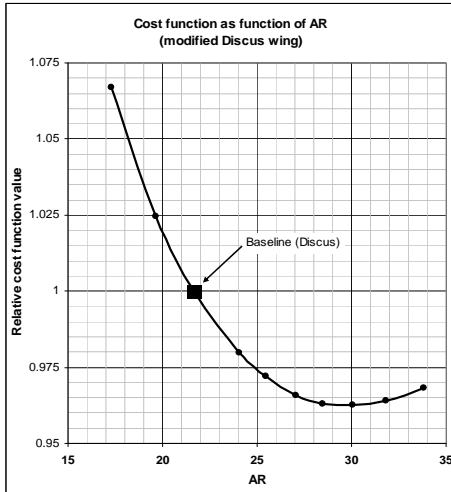


Figure 10 Aerodynamic AR optimum, according to criteria derived from the Flight Template.

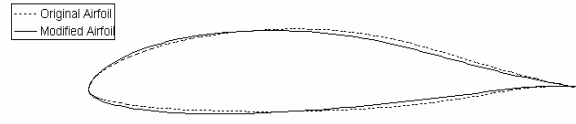


Figure 12 Airfoil geometry resulting from numerical optimization.

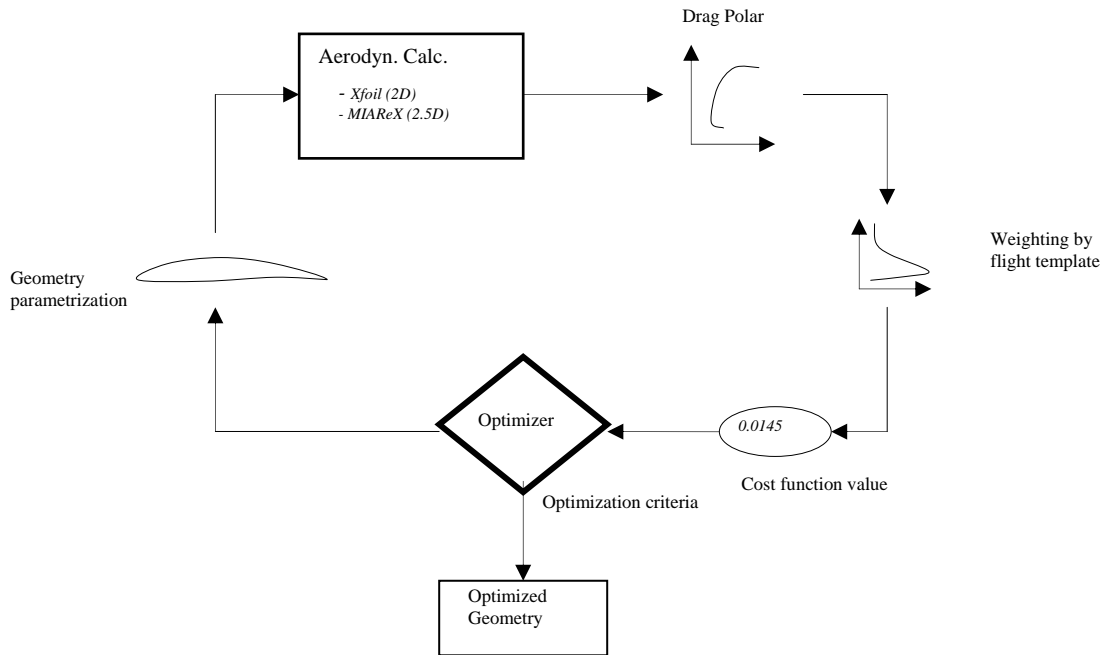


Figure 11 Numerical optimization process scheme.

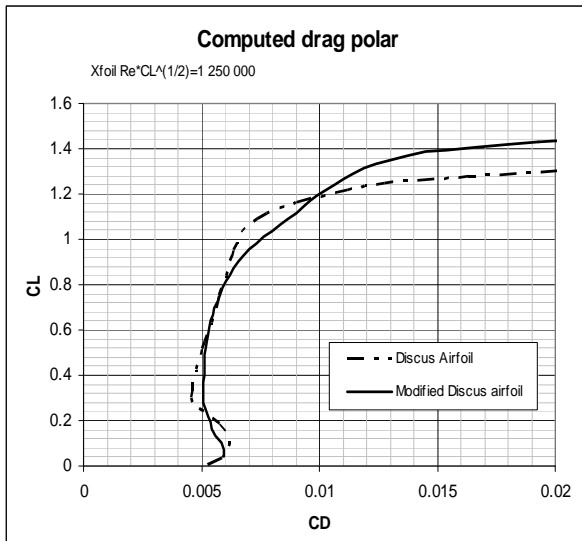


Figure 13 Drag polars.

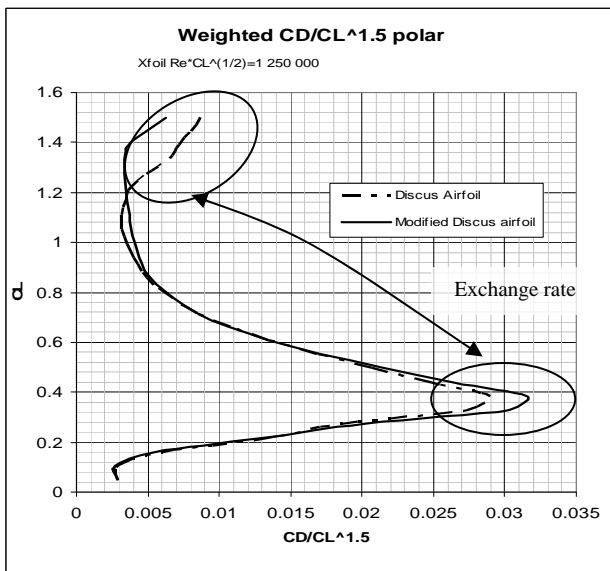


Figure 14 Weighted $C_D/C_L^{1.5}$ polars.

Table 1
"Envelope Flight Template"

CL	Flight template
0.05	0.003
0.1	0.005
0.19	0.045
0.28	0.302
0.35	0.680
0.375	0.735
0.43	0.758
0.5	0.727
0.57	0.649
0.72	0.455
0.85	0.325
1.05	0.253
1.25	0.222
1.5	0.190